



## A Modeling Method for Heterogeneous Lattice Structures based on Convolution Surface

Yuan Liu <sup>1</sup>  and Huiyuan Yang <sup>2</sup> 

<sup>1</sup> Beijing Institute of Satellite Environment and Engineering, [yuan\\_liu@buaa.edu.cn](mailto:yuan_liu@buaa.edu.cn)

<sup>2</sup> McGill University, [huiyuan.yang@mail.mcgill.ca](mailto:huiyuan.yang@mail.mcgill.ca)

Corresponding author: Yuan Liu, [yuan\\_liu@buaa.edu.cn](mailto:yuan_liu@buaa.edu.cn)

**Abstract.** Multi-material additive manufacturing (MMAM) increases much design freedom for designers to conceive heterogeneous lattice structures (HLSs) comprising the multi-phase materials with gradual variations. However, the MMAM capabilities have far outpaced the modeling capability of design systems to model and thus design novel HLS. In order to further expand the design space for the utilization of AM technology, a method of modeling HLSs with complex geometries and smooth material transitions is proposed in this paper.

**Keywords:** Heterogeneous objects modeling, Lattice structures, Convolution Surface, Additive Manufacturing.

**DOI:** <https://doi.org/10.14733/cadaps.2023.682-688>

### 1 INTRODUCTION

The areas of lattice have received considerable research attention due to their inherent advantages over foams in providing ultra-stiff and ultra-strong materials [1, 2]. Specifically, lattice have been used to replace conventional solid materials to reduce weight and enhance multi-functional properties [3, 4]. Lattice materials has a number of specialized properties, such as ultra-light, high strength ratio [5, 6], thermal insulation [7], heat exchange [8, 9], shock resistance, energy absorption [10], cooling system [11, 12] and biocompatibility [13]. It is widely used in shock/explosion systems, or as heat dissipation medium, acoustic vibration, microwave absorption structures and driving systems [14-16].

With the rapid advancement of the multi-material additive manufacturing (MMAM) technology, the heterogeneous lattice structures (HLSs) comprising the multiphase materials with gradual variations have become feasible and accessible to the industry. Varying material distribution in an object may also help designers address a broader spectrum of design challenges. HLSs often prevail over their traditional homogeneous counterparts in certain performances such as mechanical, thermal, electrical, or any combination of them. Traditional limitations, such as stress concentrations or nonuniform thermal expansion due to material incompatibility, can be avoided with a continuous gradual composition of multiple materials[17, 18].

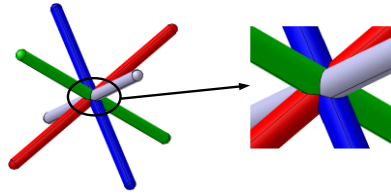


**Figure 1:** Heterogeneous Lattice structures and joint.

A Lattice unit cell consists of the lattice struct and the joint. Lattice joints (shown in Figure 1) which connect different lattice struts have a significant effect on the mechanical properties of designed lattice structures. However, currently only few research focuses on investigating how to improve the mechanical properties of lattice structures by controlling the shape or material composition of lattice joints. The sharp edges and material transitions of these joints may cause stress concentrations or material incompatibility, which may limit the further improvement of the mechanical performance of lattice structures. Simple solid Boolean operations among lattice struts have been widely used to model the shape of lattice joints. Comparing to existing Boolean operations algorithm, the novel operations and their related algorithms involving the calculation on both materials and geometries of the joint should be developed. Convolution surface is an implicit surfacing modelling technique, which is first applied to lattice design in 2017 by Yang et al[19]. It provides smooth transition in surface intersection area and has some distinctive advantages over the other conventional modeling techniques: Firstly, it can blend the surface at the connection of skeleton without creases and sharp corners. Secondly, the superposition property of convolution surfaces enables the modeling of lattice struts in a parallel manner.

In this paper, we propose a new modeling method to generate smooth joints for a given relative density and combine the multi material composition at joint. The main idea and concepts used in the proposed method will be introduced. Geometric modeling of lattice structures with convolution surfaces, and Boolean operations will be discussed in the main idea section. A short conclusion will be drawn at the end of this paper.

## 2 GEOMETRIC MODELING OF LATTICE STRUCTURES WITH CONVOLUTION SURFACES

Convolution surfaces were introduced by Bloomenthal and Shoemake [20] as a natural extension to point-based field surfaces to include higher-dimensional geometric elements.

A convolution surface is determined by a skeleton consisting of 3D points, each of which contributes to the field function according to its distance to a space point in question. Let  $\mathbf{P}_{x,y,z}$  be a space point in  $R^3$ , and let  $h: R^3 \rightarrow R$  be a geometry function that represents a modeling skeleton  $E$ :

$$h \mathbf{P} = \begin{cases} 1, & \mathbf{P} \in E \\ 0, & \mathbf{P} \notin E \end{cases} \quad (2.1)$$

Let  $f: R^3 \rightarrow R$  be a potential function that describes the field generated by a single point in the skeleton, and  $\mathbf{Q}$  be a point in the skeleton  $E$ , then the total scalar field  $F$  contributed by the skeleton at a point  $\mathbf{P}$  is the convolution of functions  $f$  and  $h$ :

$$F \mathbf{P} = \int_E h \mathbf{Q} f \mathbf{P} - \mathbf{Q} dE \quad (2.2)$$

A convolution surface with threshold  $T$  is then defined by

$$S = \{ \mathbf{P} \mid F(\mathbf{P}) - T = 0, \mathbf{P} \in R^3 \} \tag{2.3}$$

As to function  $f$  used in Eqn. (2.2), it can also be called as kernel function. In this research, we adopt the quartic polynomial as the kernel function for the convolution surface of lattice structures, and its formulation is defined as

$$f(r) = \begin{cases} \left(1 - \frac{r^2}{R^2}\right)^2, & r \leq R \\ 0, & r > R \end{cases} \tag{2.4}$$

where  $R$  is the effective radius of the kernel.

### 3 CONVOLUTION SURFACES BASED BOOLEAN OPERATIONS

In current constructive solid geometry (CSG) modeling systems, regularized Boolean operations are used to create complex objects from simple shapes (cube, sphere and cylinder etc.). Similarly, the developed Boolean operations based on the convolution surface need to be defined to create and manipulate complex heterogeneous objects models with geometric as well as material information.

We use an example in 2D for the following illustration. We denote an operator to describe the composition operation as:

$$f = G(f_1, f_2) \tag{3.1}$$

where  $G: R^2 \rightarrow R$  is a binary composition operator,  $f_1$  and  $f_2$  are field functions and  $f$  is the field function defining the resulting object.

We use Fig. 2 to illustrate the result of the union of two spheres with smooth transition region. Object  $i$  ( $i = 1, 2$ ) is defined by the field function  $f_i$ . The equation  $f_i = C$  represents object's  $i$  surface and inequalities  $f_i > C$  and  $f_i < C$  define the inside and outside of object  $i$  boundary.

The definition of operator  $G$  in each zone is shown as below:

- In zone 1,  $f_1 > 0$  and  $f_2 = 0$ . Therefore, the input of the operator is  $G(f_1, 0)$  which scales the value of function  $f_1$ .
- In zone 2,  $f_2 > 0$  and  $f_1 = 0$ . Therefore, in this area, the input of the operator is  $G(0, f_2)$  which only scales the values of function  $f_2$ .
- In zone 3,  $f_1 > 0$  and  $f_2 > 0$ . the input of the operator is  $G(f_1, f_2)$ , which is a multi-variable function. Both  $f_1$  and  $f_2$  have impacts in this region.
- In zone 4,  $f_1 = f_2 = 0$ .  $G(f_1, f_2) = G(0, 0) = C^{te}, C^{te} \in R$ .

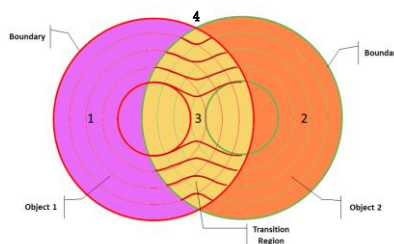


**Figure 2:** Convolution surface intersections.

In zone 1, function  $G$  scales the value of  $f_1$ . If  $G(f_1, 0) = f_1$ , operator  $G$  reproduces the metric and variation of function  $f_1$ , and the field function defined by  $f_1$  is preserved through composition. This

property eliminates the introduction of non-uniform variations in field function which can alter the regularity of the transition. Similarly, in zone 2, we also want  $G(0, f_2) = f_2$ . In zone 4, operator  $G$  is constant. It represents the outside of the resulting object boundary. It has to be continuously jointed with the other zones thus the value should be  $G(0,0) = 0$ .

A piecewise function consists of a union function and a generic arc of an ellipse function satisfies all the requirements. This function also creates an additional control over the blending region. It is based on a geometric construction of function  $G$  and a specific adaption has been used to combine unbounded implicit primitive with sharp transitions. In zone 1 and 2, the function is denoted as:

$$G(f_1, f_2) = \max(f_1, f_2) \tag{3.2}$$

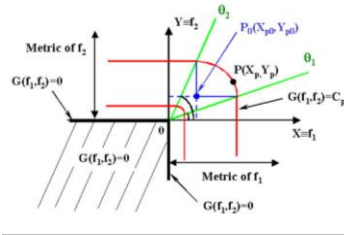


**Figure 3:** Surface intersection area formulation.

In zone 3, we propose to link the vertical iso-lines defined by  $G(f_1, 0) = f_1$  to the horizontal iso-lines defined by  $G(0, f_2) = f_2$  (shown in Figure 3) with a quarter of an ellipse defined by the following equation:

$$\frac{(f_1 - X_{p0})^2}{(C_p - X_{p0})^2} + \frac{(f_2 - Y_{p0})^2}{(C_p - Y_{p0})^2} = 1 \tag{3.3}$$

where a point  $P \in R^2$  has the coordinates  $P(f_1 = X_p, f_2 = Y_p)$  and the iso-value at this point  $G(P) = G(X_p, Y_p) = C_p$ . The center of the ellipse is  $P_0(X_{p0}, Y_{p0})$ . The junction between the two piecewise function is  $G^1$  continuous and they are both internally  $G^\infty$ .

Unknown  $X_{p0}$  and  $Y_{p0}$  can be expressed in terms of  $C_p$  and the equation is solved to compute the value of  $C_p$  returned by operator  $G$  at a point  $P(X_p, Y_p)$ .

Operator  $G$  is already designed to conserve the combined primitives' metrics outside the transition. The next step is to define the boundaries for the arc-of-an-ellipse. For this purpose, we introduce two angles  $\theta_1$  and  $\theta_2$  and the two unknowns  $X_{p0}$  and  $Y_{p0}$  can be determined by:

$$\begin{aligned} X_{p0} &= \frac{C_p}{\tan(\theta_2)} = C_p \cot(\theta_2) \\ Y_{p0} &= C_p \tan(\theta_1) \end{aligned} \tag{3.4}$$

The parameters  $\theta_1, \theta_2$  is to control the region of blending and union which can be shown in Figure 3 with  $\theta = \theta_1 = \frac{\pi}{2} - \theta_2$ .  $\theta_1, \theta_2$  control the boundaries of the blend. Therefore, a more precious version of the ellipse function is shown below:

$$\begin{aligned} G(f_1, f_2) &= \begin{cases} \max(f_1, f_2), & \text{if } f_2 \leq \tan(\theta_1)f_1 \text{ or } f_1 \leq \cot(\theta_2)f_2 \\ C: \tilde{h}_C(f_1, f_2) = 1 & \text{otherwise} \end{cases} \\ \tilde{h}_C(f_1, f_2) &= \frac{(f_1 - C \cdot \cot(\theta_2))^2}{(C - C \cdot \cot(\theta_2))^2} + \frac{(f_2 - C \cdot \tan(\theta_1))^2}{(C - C \cdot \tan(\theta_1))^2} \end{aligned} \tag{3.5}$$

where  $f_2 = \tan(\theta_1)f_1$  and  $f_1 = \cot(\theta_2)f_2$  correspond to the green lines in Figure 3.

Control points on the iso-potential surface is defined for the purpose of accurate and intuitive control. The angle  $\theta_1$  and  $\theta_2$  can be defined from the user Euclidean space  $R^3$  by selecting control points  $p_1(x_1, y_1, z_1)$  and  $p_2(x_2, y_2, z_2)$  on the combined objects' surface,  $f_1 = C$  and  $f_2 = C$ , respectively. Points  $p_1$  and  $p_2$  must be selected inside the intersection of the object's boundaries as no transition can be defined outside the boundaries. Points  $p_1 \in R^3$  and  $p_2 \in R^3$  are selected by user corresponding to points  $P_1$  and  $P_2$  in the composition surface. The expression of  $P_1$  and  $P_2$  in the combined region are  $P_1(C, f_2(p_1))$  and  $P_2(f_1(p_2), C)$  where  $f_1 = f_2 = C$ .

The construction of operator  $G$  leads to the following equation:

$$\begin{aligned} P_1 &= P_1(C, f_2(p_1)) \\ P_2 &= P_2(f_1(p_2), C) \\ \theta_1 &= \text{angle}([OX], [OP_1]), \theta_2 = \text{angle}([OX], [OP_2]) \end{aligned} \quad (3.6)$$

At point  $P(X_p, Y_p)$ :  $\theta_p = \text{angle}([OX], [OP])$ , where  $C_p$  is the solution of  $\frac{(X_p - X_{p0})^2}{(C_p - X_{p0})^2} + \frac{(Y_p - Y_{p0})^2}{(C_p - Y_{p0})^2} = 1$ , if  $\theta_p \in (\theta_1, \theta_2)$

$$G(X_p, Y_p) = \begin{cases} X_p \text{ if } Y_p = 0 \\ Y_p \text{ if } X_p = 0 \\ X_p \text{ if } \theta_p \leq \theta_1 \\ Y_p \text{ if } \theta_p \geq \theta_2 \\ C_p \text{ where } C_p \text{ is the solution of} \\ \frac{(X_p - X_{p0})^2}{(C_p - X_{p0})^2} + \frac{(Y_p - Y_{p0})^2}{(C_p - Y_{p0})^2} = 1 \\ \text{if } \theta_p \in (\theta_1, \theta_2) \end{cases} \quad (3.7)$$

#### 4 CONVOLUTION SURFACES BASED MATERIAL BLENDING

For material blending, the individual iso-surface contours are used as material source profiles and a signed distance-based material blending function is proposed to determine the local material compositions. To be specific, an important characteristic of convolution surface function is the signed distance information. The signed distance-based function calculated the value at any points representing its closet distance from the structural boundary and the sign indicates the point to be either solid (positive) or void (zero). Then, the material blending can be realized based on the signed distance information. Each level set function is treated as a material source profile. Since a signed distance field is associated with each iso-surface contour, the signed distance-based material blending can be achieved. Specific form of the convolution surface-based material blending function is demonstrated in Eqn. (4.1).

$$V_i = \frac{[1/|f_i P|]}{\sum_{j=1}^m [1/|f_j P|]} \quad (4.1)$$

where  $f_i P$  is the  $i$ th convolution surface function value at point  $P$ .  $V_i$  is the volume fraction of the material type  $i$ , which is associated to the material source profile  $f_i P$ .  $m$  is the total number of convolution surface function used to construct the contours.

As shown in Fig.4a, a design input of 3D heterogenous lattice structures, in which each strut has one of the two base materials presented by red and blue colors, respectively, is used for illustration of our modeling method. Fig. 4b shows the geometry model comparison of traditional parametric surface modelling and convolutional surface modelling. We can see that the convolutional surface modelling has a smoother transition at intersection region. One of the most important features of the convolution surface is the ability to combine the field function to form a new composed potential function and produce a smooth transition surface at intersection region.

As shown in Fig.4c, the convolution surface-based material blending result is calculated and used to conduct material modeling.

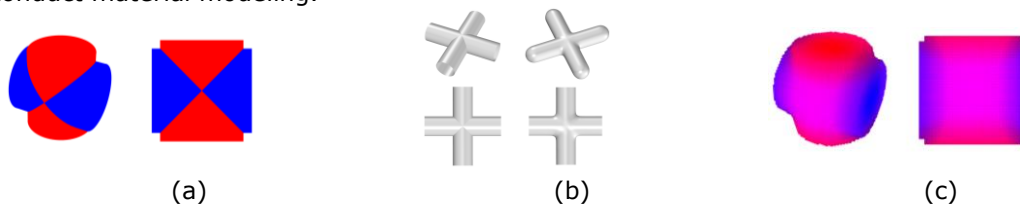


**Figure 4:** 3D case for the struts with two base materials: (a) design input, (b) comparison of parametric surface modelling and convolutional surface modelling, (c) material blending result.

## 5 CONCLUSION

In summary, we developed a new method to enhance the lattice structure formation, specifically generating smooth joint using convolution surface as well as the smooth material transitions of the joint associated with multi-material struts. This approach shows a feasible way to tackle two major design challenges: shape transition in surface modelling and multi-material composition in lattice strut joint intersections.

## 6 ACKNOWLEDGMENT

This work was supported by the Intelligent Manufacturing Special Action Plan under grant number JCKY2018203A001.

Yuan Liu, <https://orcid.org/0000-0003-3081-696X>

Huiyuan Yang, <https://orcid.org/0000-0002-8569-5846>

## REFERENCES

- [1] Li, D.; Liao, W.; Dai, N.; Dong, G.; Tang, Y.; Xie, Y. M.: Optimal design and modeling of gyroid-based functionally graded cellular structures for additive manufacturing, *Computer-Aided Design*, 104, 2018, 87-99. <https://doi.org/10.1016/j.cad.2018.06.003>
- [2] Tang, Y.; Kurtz, A.; Zhao, Y. F.: Bidirectional Evolutionary Structural Optimization (BESO) based design method for lattice structure to be fabricated by additive manufacturing, *Computer-Aided Design*, 69, 2015, 91-101. <https://doi.org/10.1016/j.cad.2015.06.001>
- [3] Cheng, L.; Liu, J.; Liang, X.; To, A. C.; Coupling lattice structure topology optimization with design-dependent feature evolution for additive manufactured heat conduction design, *Computer Methods in Applied Mechanics and Engineering*, 332, 2018, 408-439. <https://doi.org/10.1016/j.cma.2017.12.024>
- [4] Yan, D.; et al.: Soft three-dimensional network materials with rational bio-mimetic designs, *Nature communications*, 11(1), 2020, 1-11. <https://doi.org/10.1038/s41467-020-14996-5>
- [5] Clough, E. C.; Ensberg, J.; Eckel, Z. C.; Ro, C. J.; Schaedler, T. A.: Mechanical performance of hollow tetrahedral truss cores, *International Journal of Solids and Structures*, 91, 2016, 115-126. <https://doi.org/10.1016/j.ijsolstr.2016.04.006>
- [6] Liu, Y.; Zhuo, S.; Xiao, Y.; Zheng, G.; Dong, G.; Zhao, Y. F.: Rapid modeling and design optimization of multi-topology lattice structure based on unit-cell library, *Journal of Mechanical Design*, 142(9), 2020. <https://doi.org/10.1115/1.4046812>
- [7] Wadley, H. N. G.; Queheillalt, D. T.: Thermal applications of cellular lattice structures, in *Materials Science Forum*, 539-543, 2007, 242-247. <https://doi.org/10.4028/www.scientific.net/MSF.539-543.242>

- [8] Cheng, L.; Liu, J.; To, A. C.: Concurrent lattice infill with feature evolution optimization for additive manufactured heat conduction design, *Structural and Multidisciplinary Optimization*, 58(2), 2018, 511-535. <https://doi.org/10.1007/s00158-018-1905-7>
- [9] Vaissier, B.; Pernot, J.-P.; Chougrani, L.; Véron, P.: Parametric design of graded truss lattice structures for enhanced thermal dissipation, *Computer-Aided Design*, 115, 2019, 1-12.
- [10] Schaedler, T. A.; et al.: Designing metallic microlattices for energy absorber applications, *Advanced Engineering Materials*, 16(3), 2014, 276-283. <https://doi.org/10.1002/adem.201300206>
- [11] Takezawa, A.; Zhang, X.; Kato, M.; Kitamura, M.: Method to optimize an additively-manufactured functionally-graded lattice structure for effective liquid cooling, *Additive Manufacturing*, 28, 2019, 285-298. <https://doi.org/10.1016/j.addma.2019.04.004>
- [12] Tang, Y.; Gao, Z.; Zhao, Y. F.: Design of conformal porous structures for the cooling system of an injection mold fabricated by Additive Manufacturing Process, *Journal of Mechanical Design*, 141(10), 2019, 101702. <https://doi.org/10.1115/1.4043680>
- [13] Puppi, D.; et al.: Additive manufacturing of wet-spun polymeric scaffolds for bone tissue engineering, *Biomedical Microdevices*, 14(6), 2012, 1115-1127. <https://doi.org/10.1007/s10544-012-9677-0>
- [14] Varanasi, S.; Bolton, J. S.; Siegmund, T. H.; Cipra, R. J.: The low frequency performance of metamaterial barriers based on cellular structures, *Applied Acoustics*, 74(4), 2013, 485-495. <https://doi.org/10.1016/j.apacoust.2012.09.008>
- [15] Zhang, Q.; Zhang, F.; Xu, X.; Zhou, C.; Lin, D.: Three-Dimensional Printing Hollow Polymer Template-Mediated Graphene Lattices with Tailorable Architectures and Multifunctional Properties, *ACS Nano*, Article 12(2), 2018, 1096-1106. <https://doi.org/10.1021/acsnano.7b06095>
- [16] Egan, P. F.; Bauer, I.; Shea, K.; Ferguson, S. J.: Mechanics of three-dimensional printed lattices for biomedical devices, *Journal of Mechanical Design*, 141(3), 031703, 2019. <https://doi.org/10.1115/1.4042213>
- [17] Liu, Y.; Yang, H.; Zhao, Y. F.; Zheng, G.: A heterogeneous lattice structure modeling technique supported by multiquadric radial basis function networks, *Journal of Computational Design and Engineering*, 9(1), 2022, 68-81. <https://doi.org/10.1093/jcde/qwab069>
- [18] Liu, Y.; Zheng, G.; Letov, N.; Zhao, Y. F.: A Survey of Modeling and Optimization Methods for Multi-Scale Heterogeneous Lattice Structures, *Journal of Mechanical Design*, 143(4), 040803, 2021. <https://doi.org/10.1115/1.4047917>
- [19] Yang, H.; Zhao, Y.: A new method for designing porous implant, in *DS 87-5 Proceedings of the 21st International Conference on Engineering Design (ICED 17) Vol 5: Design for X, Design to X*, Vancouver, Canada, 21-25.08. 2017, 2017, pp. 337-344.
- [20] Bloomenthal, J.; Shoemake, K.: Convolution surfaces, in *Proceedings of the 18th annual conference on Computer graphics and interactive techniques*, 1991, 251-256. <https://doi.org/10.1115/1.4047917>